Ab initio pseudopotential studies of cubic BC_2N under high pressure

2005 J. Phys.: Condens. Matter 17 3211

(http://iopscience.iop.org/0953-8984/17/21/015)

INSTITUTE OF PHYSICS PUBLISHING JOURNAL OF PHYSICS: CONDENSED MATTER

J. Phys.: Condens. Matter **17** (2005) 3211–3220 doi:10.1088/0953-8984/17/21/015

Ab initio pseudopotential studies of cubic BC_2N under high pressure

Zicheng Pan[1], **Hong Sun**[1,2] **and Changfeng Chen**[2]

[1] Department of Physics, Shanghai Jiao Tong University, Shanghai 200030, People's Republic of China
[2] Department of Physics and High Pressure Science and Engineering Center, University of Nevada, Las Vegas, NV 89154, USA

Received 13 December 2004, in final form 20 April 2005
Published 13 May 2005
Online at stacks.iop.org/JPhysCM/17/3211

Abstract

We present the results of a systematic study of the structural, electronic, and vibrational properties of various cubic BC_2N phases under high pressure. *Ab initio* pseudopotential total-energy and phonon calculations have been carried out to examine the changes in the structural parameters, bonding behaviours, band structures, and dynamic instabilities caused by phonon softening in these phases. We find that an experimentally synthesized high-density phase of cubic BC_2N exhibits outstanding stability in the structural and electronic properties up to very high pressures. On the other hand, another experimentally identified phase with lower density and lower symmetry undergoes a dramatic structural transformation with a volume and bond-length collapse and a concomitant semi-metal to semiconductor transition. A third phase is predicted to be favourable over the above-mentioned lower-density phase by the enthalpy calculations. However, the dynamic phonon calculations reveal that it develops imaginary phonon modes and, therefore, is unstable in the experimental pressure range. The calculations indicate that its synthesis may be achieved at reduced pressures. These results provide a comprehensive understanding for the high-pressure behaviour of the cubic BC_2N phases and reveal their interesting properties that can be verified by experiments.

1. Introduction

The synthesis and characterization of ternary B–C–N compounds have attracted considerable interest in recent years due to their outstanding performance properties, such as high melting temperatures, large bulk and shear moduli, and high thermal coefficients, which make them a potential new generation of so-called superhard materials with wide applications in science and technology. Among various ternary B–C–N systems, cubic BC_2N phases have received special attention since they are most frequently prepared in experiments and display a wide range of diverse results on structural forms and properties [1–3]. In particular, x-ray diffraction data

have revealed the existence of two distinct cubic BC_2N phases: (i) a high-density phase [1, 2] with the lattice constant close to that predicted based on the ideal mixing of diamond and cubic BN and (ii) a lower-density phase [3] with the lattice constant 1.4% larger than that of the ideal mixing. Previous theoretical studies [4] suggest that this diversity reflects the fact that these phases are different metastable structures of cubic BC_2N. One area of research that is of great importance to the understanding of the synthesis and characterization of these phases is a systematic study of their high-pressure behaviour. It was recently shown [5] that different starting material forms may lead to diverging synthesis routes and yield end products with very different physical properties. This provides an explanation for the experimentally observed variations in the structural characteristics of the synthesized cubic BC_2N phases. These successful identifications of the experimentally observed structures with distinct physical properties point to the need for a detailed investigation of their high-pressure behaviour, which will provide a better understanding of the physical properties that are important for applications of the cubic BC_2N phases as superhard materials.

In this paper, we present the results of a study of the structural, electronic and vibrational properties of various BC_2N phases at high pressure using *ab initio* pseudopotential total-energy and dynamic phonon calculations. The evolution of the structural parameters, the band structures, and the dynamic phonon instabilities are examined in detail. This study is aimed at providing a better understanding of the synthesized superhard cubic BC_2N. We are interested in the high-pressure behaviour of physical properties such as the expected volume and bond-length contractions and the changes in local bonding environments, the resultant variations in the electronic band structure, particularly the nature of the bandgap, and the shifts in phonon frequencies. The calculated results show interesting evolutions of the electronic band structure in close connection to the pressure driven changes in the bonding environment and the symmetry of the cubic BC_2N structures. We also show the important role played by the dynamic phonon instability in the synthesis process.

The rest of the paper is organized as follows. Section 2 describes the *ab initio* pseudopotential total-energy and dynamic phonon calculations used in the present work, and the structural model for the cubic BC_2N phases. Section 3 shows the calculated results and the discussion on the variations of the physical properties in response to pressure and their experimental implications. Finally, a summary is presented in section 4.

2. Method of calculation

The total energy of the cubic BC_2N phases is computed using the local-density-approximation (LDA) pseudopotential scheme with a plane-wave basis set [6–8], a cut-off energy of 80 Ryd and an $8 \times 8 \times 8$ Monkhorst–Pack k-point grid. The norm-conserving Troullier–Martins pseudopotentials [9] were used with cut-off radii of 1.3, 1.3, and 1.5 au for N, C, and B, respectively. The exchange–correlation functional of Ceperley and Alder [7] as parametrized by Perdew and Zunger [10] was used. The energy of the structures is minimized by relaxing the structural parameters using a quasi-Newton method [11]. Phonon modes of the crystal structure were calculated with the linear response theory [12] using the ABINIT code for the equilibrium structures obtained after the structural relaxation. This approach has been applied to systems containing B, C, and N, including layered graphitic structures, with good accuracies on structural parameters and phonon frequencies [4, 13].

In the present work, we adopt an eight-atom zinc-blende-structured unit cell used previously [4] in the study of the equilibrium structures of the cubic BC_2N phases at zero pressure. Out of a total of $8!/(2!)^2 4! = 420$ different configurations only seven are topologically different, due to the high symmetry of the zinc-blende-structured lattice. These

Table 1. Calculated structural parameters and enthalpy for the seven c-BC_2N phases at 100 GPa.

Structure	1	2	3	4	5	6	7
a (Å)	3.360	3.359	3.358	3.373	3.362	3.375	3.283
b (Å)	3.403	3.359	3.429	3.389	3.422	3.375	3.283
c (Å)	3.360	3.403	3.358	3.373	3.362	3.395	3.891
α (deg)	90.18	90.00	90.00	89.99	89.85	89.84	81.60
β (deg)	90.00	90.00	90.00	90.07	90.22	89.84	98.40
γ (deg)	90.00	90.00	90.00	90.01	90.15	89.82	94.30
$\overline{a}$ (Å)	3.374	3.374	3.381	3.379	3.381	3.382	3.443
H (eV/atom)	−161.83	−161.83	−161.34	−161.47	−161.47	−161.36	−161.41

seven structures are numbered according to the increasing number of B–B and N–N bonds, which are found to be energetically unfavourable for the formation of the cubic BC_2N phases. After full structural relaxations, cubic BC_2N numbers 1–4 maintain the zinc-blende structure with a full covalent bonding and symmetry close to the ideal cubic lattice. Meanwhile, BC_2N numbers 5 and 6 each have a broken N–N bond, and number 7 has two broken bonds, one N–N and one B–B, in the structure. These different bonding characters clearly manifest themselves in their high-pressure behaviour as will be seen below.

3. Results and discussion

Table 1 lists the fully relaxed structural parameters of the seven c-BC_2N phases at 100 GPa obtained from the *ab initio* calculations, together with the calculated enthalpy $H = E + pV$, where E is the total energy, p the applied pressure, and V the volume, and the average lattice constant $\overline{a}$ defined as the cubic root of the volume of the unit cell. These results should be compared to those at $p = 0$ [4] to see the effect of the applied pressure. The average lattice constant is useful in making comparison with experimental data [1–3] where the peak broadening in the angle dispersive x-ray measurements introduces ambiguities into the structural assignment; in particular, deviations from the ideal cubic lattice structure (i.e., differences among a, b, and c) are not distinguished in the experiments. Instead, a single lattice constant is extracted with the assumption of the ideal cubic symmetry, which should be compared with the calculated average lattice constant $\overline{a}$. Among these seven structures, BC_2N-1 (BC_2N-2 is practically degenerate with and indistinguishable from BC_2N-1 in most aspects) and BC_2N-5 have been suggested [4] to be the experimentally obtained high-density and lower-density phase, respectively. These structural assignments have been supported by the good agreement between the calculated and measured structural and elastic parameters [4, 5] and by the enthalpy–pressure calculations and the dynamic phonon calculations [5] in comparison with a Brillouin scattering experiment [14]. The calculated enthalpy indicates that BC_2N-1 (also BC_2N-2 that remains nearly degenerate with BC_2N-1 over the entire pressure range) remains the most stable cubic BC_2N phase at high pressure (up to at least 400 GPa according to our calculations). Meanwhile, despite its higher energy/enthalpy, BC_2N-5 (which is close in structural characteristics but stays consistently lower in enthalpy by 0.1 eV/atom compared to BC_2N-6) also maintains its overall structural stability under pressure without a transition into other structures, although a pressure driven bond-length (or volume) collapse does occur at 44–45 GPa (see below). From the structural data in table 1 it is seen that applied pressure compresses the lattice constant and reduces the structural deviations from ideal cubic symmetry as expected. At 100 GPa, only BC_2N-7 still has significant deviations in the structural parameters from ideal cubic symmetry. At further increased pressure above

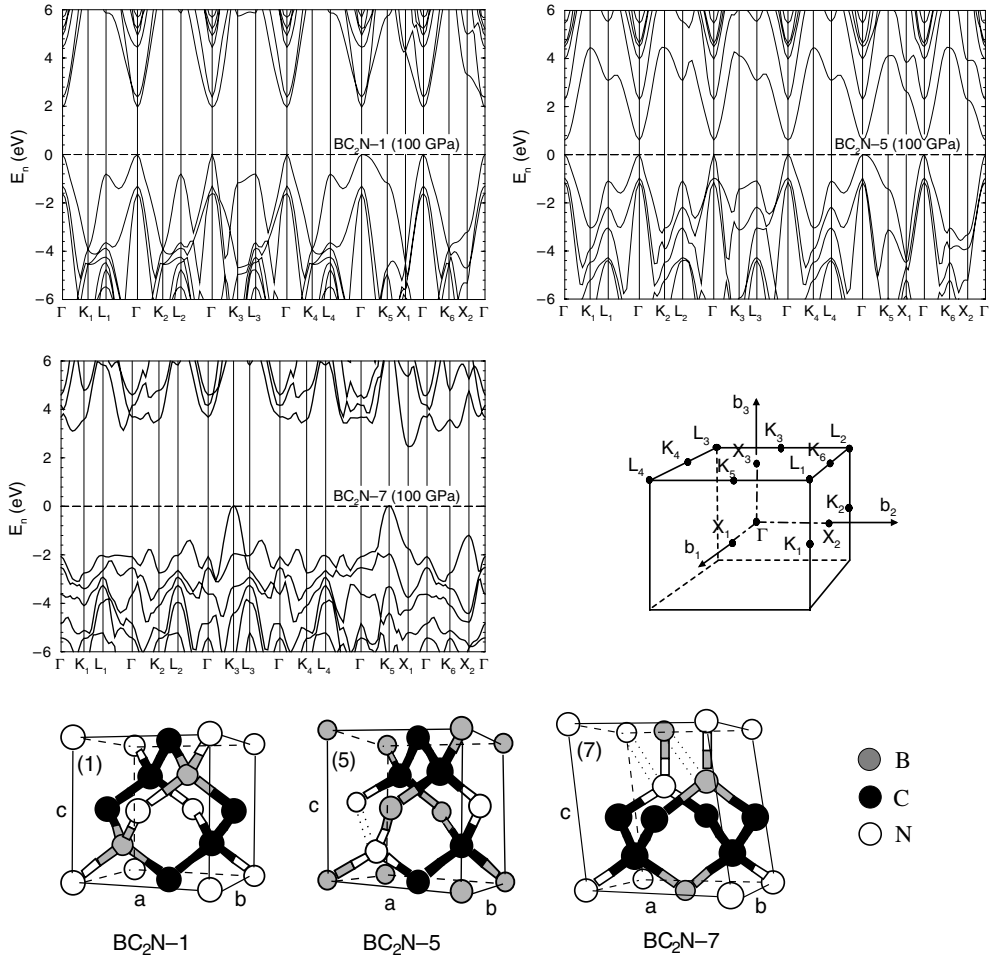

Figure 1. Calculated band structures of selected BC_2N phases (BC_2N-1, 5, and 7, respectively, as indicated) at 100 GPa. The definition of the *k* points in the reciprocal lattice is shown in the middle right of the figure. The equilibrium structures of the BC_2N-1, 5, and 7 phases are given at the bottom of the figure (see [4] for more BC_2N structures). The broken covalent bonds between N–N and B–B are represented by the dashed lines.

100 GPa (calculations were performed up to 400 GPa), no major changes are observed in the structural and electronic properties, other than the expected further slow compression in the lattice constants and the enhancement of the electronic bandgap.

To examine the effects of these pressure driven structural changes on the electronic properties, we have calculated the electronic band structure for the three representative structures, BC_2N-1, BC_2N-5, and BC_2N-7 (see figure 1). The first two structures represent the experimentally observed high- and low-density cubic phase as mentioned above, while BC_2N-7 is an interesting case where dynamic phonon instabilities may have prevented its synthesis in the reported experimental pressure range. We will show below that at reduced pressures the synthesis of this phase may still be achievable. The calculated electronic band structures of the three selected cubic BC_2N structures at 100 GPa are shown in figure 1 for a comparative study of the pressure effect on the electronic properties (see [4] for the zero-

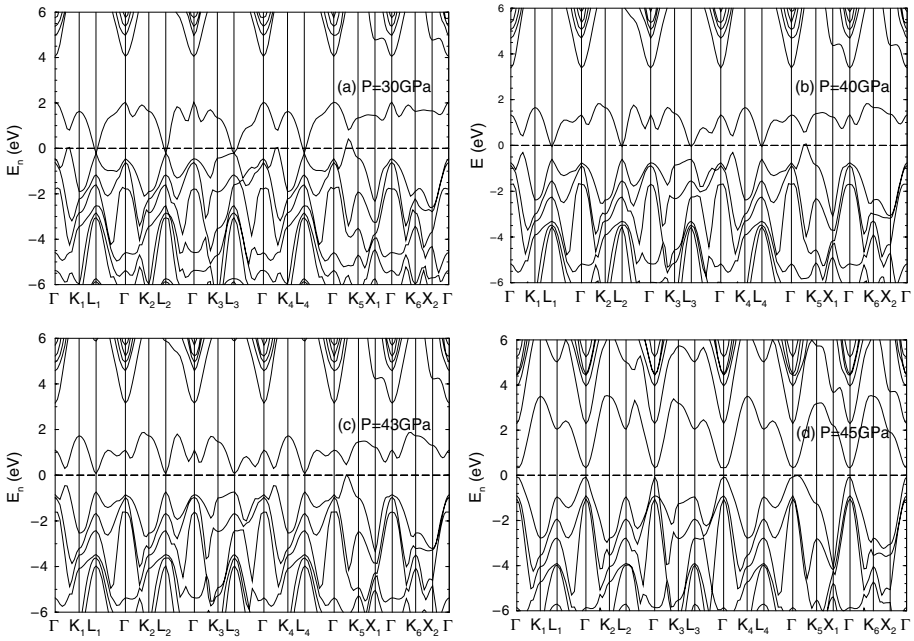

Figure 2. Calculated band structures of BC_2N-5 at selected pressures.

pressure band structures). Pressure induced enhancement of the bandgap is clearly seen in all cases. This can be understood as a result of the stronger repulsive interactions due to the closer atomic positions in the compressed phases. Of particular interest is BC_2N-5, which is a (LDA) semimetal in the absence of pressure and turns into a direct bandgap semiconductor at high pressure. To further elucidate the process and the underlying mechanism for this transition, we have carried out additional calculations of the band structure in the intermediate-pressure range. Figure 2 shows the band structure at selected pressure points below and above the pressure where the (LDA) bandgap opens up. It is noticed that up to 30 GPa the conduction and valence band crossings are all located at the same k-points at the Fermi level (see figure 2(a)). This situation is reminiscent of that in graphite [15], which is a semimetal with similar band structure arrangements near the Fermi level. As pressure further increases, the conduction and valence band crossings begin to open up, and the conduction band minimum and the valence band maximum start to shift apart; at pressures near 40 GPa this shift becomes quite significant (see figure 2(b)). This may allow a bandgap to open in more accurate calculations using, for example, the GW scheme [16]. Consequently, the present calculations may have overestimated the pressure for the semimetal to semiconductor transition. An interesting observation of the calculated electronic band structure as a function of pressure is that the semiconducting phase initially has an indirect bandgap in the pressure range of 40–45 GPa (see figure 2(c) for the band structure at $P = 43$ GPa) and then turns into a direct gap semiconductor starting at 45 GPa (see figure 2(d)). This transition to the direct bandgap can be understood as a consequence of the restoration of the cubic symmetry of the system at the higher pressure. Above 45 GPa the bandgap gradually increases at a slow pace that is consistent with the slow change in the structural parameters at higher pressures (see below).

To understand the relation between the electronic band structure and the structural variations, we examine the pressure driven structural changes in BC_2N-1, 5, and 7. The

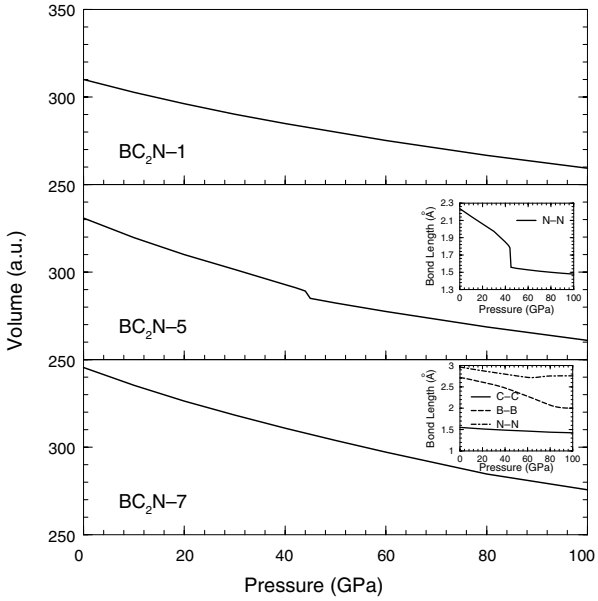

Figure 3. Calculated volume compression results for BC_2N-1, 5, and 7. The insets show the contraction of selected bond lengths in BC_2N-5 and 7.

calculated equation of state (volume compression) and selected average bond lengths for these three phases up to 100 GPa are shown in figure 3. It is seen that the volume (and the bond length, not shown here) contraction is slow and smooth for the high-density phase BC_2N-1. Similar behaviour (not shown here) has been obtained for BC_2N-2, 3, and 4 due to their higher densities and fully covalent bonded environments. These results indicate high stability and low compressibility of these structures. It explains the very small magnitude of the bandgap enhancement at high pressure for BC_2N-1 shown in figure 1. Meanwhile, the initial contraction is much faster for the lower-density phase BC_2N-5 (similar behaviour for BC_2N-6; not shown here). At 44–45 GPa, a 2% volume collapse occurs; a close examination of the individual bonds reveals a much more dramatic 14% collapse in the bond length of the originally broken covalent N–N bond. At higher pressure, BC_2N-5 reaches a density very close to that of BC_2N-1 and further contraction of the volume (and the bong lengths) also becomes smooth and slow, similar to that of BC_2N-1. From the data listed in table 1 it is also seen that the structure of BC_2N-5 is much closer to the ideal cubic symmetry at high pressure (100 GPa) than it is at $p = 0$ GPa [4]. This restoration of the covalent N–N bond and the overall cubic symmetry are the underlying driving force for the transition from an indirect-gap semiconductor to a direct-gap semiconductor in BC_2N-5. It is noticed that the N–N and B–B bonds in BC_2N-7 still remain broken even at 100 GPa due to the much stronger repulsion than that in BC_2N-5 or BC_2N-6 which has only one broken bond each at low pressure. As a result of this large deviation from the cubic symmetry (see also the data in table 1) BC_2N-7 remains an indirect-gap semiconductor at 100 GPa (see figure 1). Another important factor here is the change in the topology of the local bonding character, for example, from the sp^2 bonding associated with the originally broken N–N bond to sp^3 bonding in the compressed high-symmetry structure in BC_2N-5. It is determined by examining the angles between the two adjacent bonds (excluding the N–N bond) connected to the same N atom, which change from 120° to 109.5°, while the angles between the N–N bond and its adjacent bonds change from 90° to 109.5°.

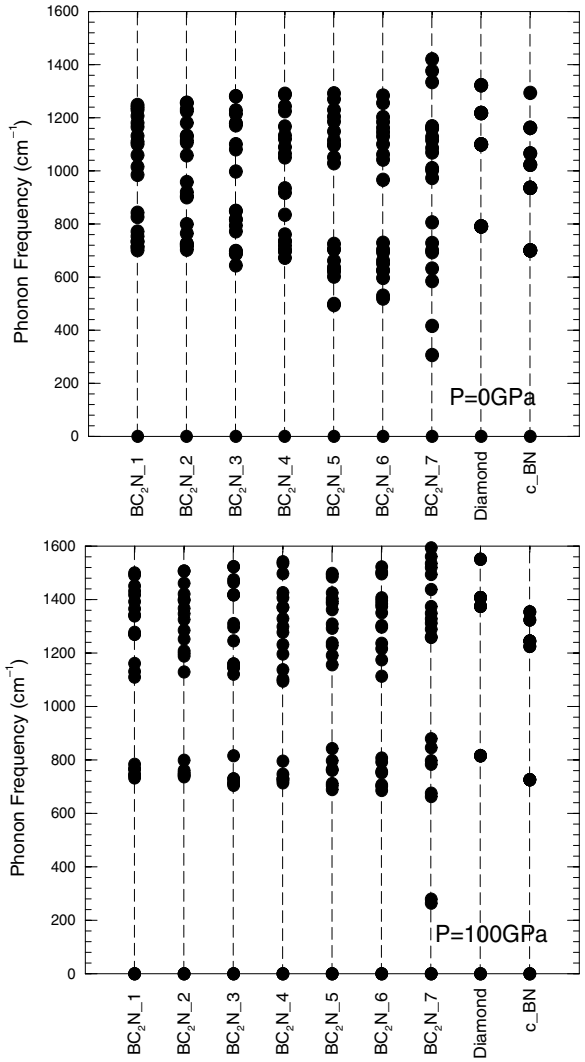

Figure 4. Calculated phonon (Γ) frequencies for the seven BC_2N phases at zero and 100 GPa. The calculated results for diamond and cubic BN are also shown for comparison.

Apart from the electronic properties, the phonon frequencies of the cubic BC_2N phases also depend sensitively on the structural changes driven by external pressure. In figure 4, we plot the calculated phonon frequencies at the Γ point for the seven cubic BC_2N structures at zero and 100 GPa. For the purpose of comparison, the calculated phonon frequencies at the Γ point for diamond and c-BN are also included. At zero pressure, the distribution of phonon frequencies at the Γ point can be classified into three groups: (i) BC_2N-1–BC_2N-4, which contain no broken covalent bonds; the phonon frequencies of this group are similar to those of diamond and c-BN; (ii) BC_2N-5 and BC_2N-6, which contain one N–N broken covalent bond; the (lowest) optical phonon frequencies at Γ are shifted downwards by about 200 cm^{-1}; (iii) BC_2N-7, which contains two broken covalent bonds, one N–N and one B–B; the (lowest) optical phonon frequencies at Γ are shifted downwards by another 200 cm^{-1}. In combination

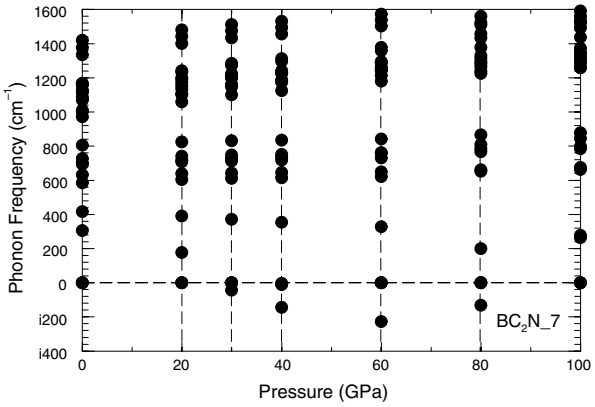

Figure 5. Calculated phonon (Γ) frequencies for BC_2N-7 at selected pressures.

with optical (Raman and/or infrared) spectroscopy experiments, these calculated systematic shifts of frequencies can be used as an additional valuable tool to identify various cubic BC_2N structures that are nearly degenerate in many aspects and hard to distinguish [4]. Meanwhile, at 100 GPa the phonon frequency distributions of all the cubic BC_2N structures, with the only exception of BC_2N-7, are very close, due to the restoration of the broken N–N covalent bonds. This is fully consistent with the structural data shown in table 1.

The exceptional case of BC_2N-7 deserves more careful attention. In figure 5, we plot the calculated phonon frequencies (Γ) of BC_2N-7 at selected pressures from zero to 100 GPa. It is noted that BC_2N-7 becomes unstable around 30 GPa, where imaginary phonon frequencies (at Γ) start to develop. These phonon softening modes persist over a large pressure range between 30 and 100 GPa. This offers an explanation for the somewhat puzzling observation in the synthesis of cubic BC_2N. From table 2 of [4] it is seen that structure 7 has the third lowest calculated energy after BC_2N-1 and BC_2N-2. The latter pair have been identified [4, 5] to be the experimentally observed high-density cubic phase [1, 2]. However, the experimentally observed lower-density cubic phase [3] has not been assigned to the structure of BC_2N-7, but that of BC_2N-5, that is higher in energy. The discovery of the dynamic phonon instability presented in this paper not only explains its absence in the reported experiments, but also points to possible synthesis of this structure at reduced (below 20 GPa) pressures. It should be noted though that the identification of the proper starting material form to reduce the kinetic barrier along the synthesis route remains an important open issue.

Finally we remark on the effect of the structural deviations from the ideal cubic symmetry in the c-BC_2N phases. These phases have nearly cubic lattice structures but deviate from the ideal cubic arrangement, especially at low pressure, as demonstrated by the structural parameters shown in table 1. Moreover, due to the non-uniform interatomic interactions in these ternary phases, in particular the strongly repulsive N–N and B–B interactions, the distributions of atomic positions further deviate from the ideal zinc-blende arrangement. These deviations from the ideal cubic symmetry have important implications for the physical properties of the cubic BC_2N phases. For example, simple textbook relations between acoustic sound velocities and lattice parameters plus a few high-symmetry elastic moduli can no longer be applied here; instead, a full calculation incorporating all (21 in the present case) elastic moduli and structural parameters are required to obtain the acoustic sound velocities. Calculations of full phonon bands using first-principles approaches are needed to obtain reliable results on longitudinal and transverse sound velocities [5]. Another consequence of the symmetry reduction is the lack

of phonon softening at the peak of the stress–strain curve [17]. Solving the standard dynamic equation [18] governing the elastic wave in solids with the ideal cubic symmetry leads to the conclusion that there exists a longitudinal acoustic mode $\omega^2 = 0$, namely phonon softening, in the cubic system at the peak stress. However, real materials under stress rarely retain the ideal cubic symmetry. As a result, acoustic phonon bands will not develop zero phonon modes (i.e., softening) at the peak stress as recently demonstrated [17] for strained c-BC_2N.

4. Summary

In summary, we have carried out systematic *ab initio* pseudopotential total-energy and dynamic phonon calculations to study the high-pressure behaviour of the cubic BC_2N phases. We have found rich variations among different BC_2N structures in their structural, electronic, and vibrational properties and presented detailed results on the pressure driven evolution of these properties. A high-density phase (BC_2N-1 or 2) exhibits high stability and low compressibility under pressure, while a lower-density phase (BC_2N-5) displays a dramatic pressure induced bond-length (and volume) collapse around 44–45 GPa and a concomitant transition from a semi-metal to a semiconductor. The bond-length collapse leads to the restoration of the originally broken covalent N–N bond and the overall symmetry of the structure, which, in turn, results in a transition from an indirect bandgap semiconducting phase to a direct bandgap phase. Another lower-density phase (BC_2N-7) exhibits intriguing dynamic phonon instabilities, indicated by the development of imaginary phonon modes, in the pressure range corresponding to the reported experimental synthesis conditions. At reduced synthesis pressures, coupled with a proper choice of starting material form to minimize the kinetic barrier, the realization of this interesting structural phase may be possible. It is worth noting that the dynamic phonon calculations also provide, in combination with optical (Raman and/or infrared) spectroscopy experiments, a valuable tool for the structural characterization and distinction of these otherwise very close (both energetically and structurally) material forms. These calculated high-pressure behaviours of the cubic BC_2N phases can be directly verified by experiments.

Finally, it should be noted that the LDA calculations reported in the present work typically underestimate bond lengths and bandgaps and overestimate binding energy. Consequently, some quantitative aspects in the reported results may be subject to correction by better quality calculations in the future.

Acknowledgments

We thank Yusheng Zhao for valuable discussions on the experimental aspects of BC_2N. This work was supported in part by the Open Fund of the Grid Computing Center at the Shanghai Jiao Tong University, and we appreciate the use of the IBM p690 supercomputer at the Center. Work at the University of Nevada, Las Vegas, was supported by the Department of Energy under cooperative agreement DE-FC52-01NV14049.

References

[1] Knittle E, Kaner R B, Jeanloz R and Cohen M L 1995 *Phys. Rev.* B **51** 12149
[2] Zhao Y S, He D W, Maemen L L, Shen T D, Schwarz R B, Zhu Y, Bish D L, Huang J, Zhang J, Shen G, Qian J and Zerda T W 2002 *J. Mater. Res.* **17** 3139
[3] Solozhenko V L, Andrault D, Fiquet G, Mezouar M and Rubie D C 2001 *Appl. Phys. Lett.* **78** 1385
[4] Sun H, Jhi S H, Roundy D, Cohen M L and Louie S G 2001 *Phys. Rev.* B **64** 094108

[5] Pan Z C, Sun H and Chen C F 2004 *Phys. Rev.* B **70** 174115
[6] Ihm J, Zunger A and Cohen M L 1979 *J. Phys. C: Solid State Phys.* **12** 4409
[7] Ceperley D M and Alder B J 1980 *Phys. Rev. Lett.* **45** 566
[8] Cohen M L 1982 *Phys. Scr.* T **1** 5
[9] Troullier N and Martins J L 1991 *Phys. Rev.* B **43** 1993
[10] Perdew J P and Zunger A 1981 *Phys. Rev.* B **23** 5048
[11] Pfrommer B G, Cote M, Louie S G and Cohen M L 1997 *J. Comput. Phys.* **131** 233
[12] Gonze X 1997 *Phys. Rev.* B **55** 10337
Gonze X and Lee C 1997 *Phys. Rev.* B **55** 10355
[13] Sun H, Ribeiro F J, Li J L, Roundy D, Cohen M L and Louie S G 2004 *Phys. Rev.* B **69** 024110
[14] Tkachev S N, Solozhenko V L, Zinin P V, Manghnani M H and Ming L C 2003 *Phys. Rev.* B **68** 052104
[15] Boettger J C 1997 *Phys. Rev.* B **55** 11202
[16] Fleszar A 2001 *Phys. Rev.* B **64** 245204
[17] Zhang Y, Sun H and Chen C F 2004 *Phys. Rev. Lett.* **93** 195504
[18] Auld B A 1973 *Acoustic Fields and Waves in Solids* vol 1 (New York: Wiley) p 58 and p 211